Integration of a 3D-Printed Façade Unit in a Curtain Wall System: Prototyping and Assessment

Francesco Milano[1*], Ringo Perez Gamote[2], Nik Eftekhar Olivo[3], Valeria Piccioni[4], Po Yen Chen, Caitlin Gallagher, Arno Schlueter[4], Benjamin Dillenburger[3], Andreas Luible[2], Fabio Gramazio[1], Matthias Kohler[1*]

* Corresponding author: milano@arch.ethz.ch
1 Gramazio&Kohler Research, ITA, ETH Zurich, Switzerland
2 HSLU, Luzern, Switzerland
3 Digital Building Technologies, ITA, ETH Zurich, Switzerland
4 Architecture and Building Systems, ITA, ETH Zurich, Switzerland

Abstract

Plastic materials, known for their lightweight, formability, transparency, and durability, are the state of the art for building façade applications. Recent advances in Large-Scale Robotic 3D Printing (LSR3DP) have enabled the production of bespoke, translucent façade components. While research has largely focused on individual panel properties, there is a gap in developing a comprehensive strategy for integrating these components into a complete façade system. This paper explores the potential of combining custom 3D-printed façade elements with standard curtain wall connections. Quantitative analysis involves constructing and testing a 1 m x 1 m LSR3DP façade assembly for air and water tightness, benchmarking its performance against a conventional curtain wall. Qualitatively, the approach is evaluated through a mock-up, highlighting the architectural possibilities of blending standard and non-standard façade elements. The findings demonstrate that this hybrid system is both technically viable and opens new design possibilities for architects and façade engineers.

Keywords

Façade design, 3D printing, Computational design, Digital fabrication

DOI

http://doi.org/10.47982/jfde.2024.325

1 INTRODUCTION

1.1 BACKGROUND

Plastics are a broad set of synthetic materials that use polymers as the main ingredient (Engelsmann et al., 2010). They are characterised by specific properties – such as lightweight, good weather resistance, high strength, and excellent forming characteristics – which make them particularly interesting for building façade applications (Herzog et al., 2004). Plastic façades have been the state of the art in building and construction since the 1950s and remain a focus of ongoing innovation. Over the past decade, different research projects emerged exploring the possibility of using 3D printing to produce building façade components (Leschok et al., 2023) (Naboni & Jakica, 2022) (Mungenast, 2019) (Fleckenstein et al., 2023). Within this field, a research subset consists of using Large-Scale Robotic 3D Printing (LSR3DP) to produce bespoke, translucent façade components out of plastic (Seshadri et al., 2021) (Cheibas, 2023) (Cheibas, Perez Gamote, et al., 2023) (Cheibas, Piccioni, et al., 2023) (Cheibas, Lloret-Fritschi, et al., 2023) (Piccioni, Leschok, Lydon, et al., 2023) (Piccioni, Leschok, Grobe, et al., 2023). LSR3DP consists of a fused deposition modelling (FDM) system composed of a material extruder mounted on the flange of a 6-axis robotic arm. This technology can produce large-scale components and is characterised by great kinematic possibilities compared to cartesian alternatives (Al Jassmi et al., 2018). Compared to other plastic processing techniques (standard extrusion, moulding, cutting, and milling), LSR3DP entails multiple advantages. (i) It can produce bespoke geometries at no extra cost. (ii) It is fully automatic and, therefore, not labour-intensive. (iii) It is materially effective, being additive rather than subtractive. (iv) It is suitable for producing complex geometries (Strauß, 2013). Different experiments on translucent LSR3DP façade components have already been conducted. Next to the opportunity to expand design possibilities and create novel architectural effects, researchers have been focusing on how this technology can be used to foster efficient façade design, creating highly integrated systems tailored to specific climatic contingencies. In most cases, parameters such as the global geometry or the level of transparency are tuned to optimise solar gain, light transmission, and glare, while the internal articulation is designed to regulate heat and load transfer.

1.2 STATE OF THE ART

Seshadri et al. propose an experimental methodology to optimise the outside geometry of a façade module in relation to solar radiation (Seshadri et al., 2021). The process is based on parametric design, daylight simulation, and topology optimisation. Piccioni et al. explore the possibility of selectively admitting or blocking solar radiation in a translucent polymeric panel by adjusting different parameters in the 3D printing process. The study demonstrates that by varying printing speed, printing temperature, and layer height, optical properties like different levels of transparency, translucency, and haze can be obtained (Piccioni, Leschok, Grobe, et al., 2023). Piccioni et al. also explore the effect of a 3D-printed component's internal geometry on its thermal insulation properties. The study demonstrates how thermal transmittance changes (ranging from 1.7 to 1 W/m^2K) as a function of the internal cavity distribution and size (Piccioni, Leschok, Lydon, et al., 2023). Cheibas et al. propose a conceptual workflow in which the global geometry of a façade, 3D printed out of translucent thermoplastics, is tailored to integrate environmental parameters (Cheibas, Lloret-Fritschi, et al., 2023). Another study demonstrates how different 3DP patterns produced on the panel's outside surface can influence the levels of translucency and, therefore, be used to create bespoke daylight and shading effects (Cheibas, Piccioni, et al., 2023).

1.3 RESEARCH GAP

To date, studies on translucent LSR3DP façades have primarily concentrated on designing and evaluating individual façade components, but more development needs to be done in producing a comprehensive façade construction strategy. In particular, limited developments exist on the interface between neighbouring components and how such a façade would coherently integrate into the larger building ecosystem (load-bearing structure, slabs, roof). Cheibas et al. explored an integrated snap connection strategy inspired by classic unitised curtain walls (Cheibas, Perez Gamote, et al., 2023) (Cheibas, 2023). The exploration was followed by producing a façade prototype, which was tested for air permeability and water tightness. The prototype didn't meet the requirements of the current standards and could not be classified. From a fabrication perspective, integrating performative male-female connections along the edges of an LSR3DP panel is challenging due to the technology's low resolution and the impossibility of creating temporary supports. The problem of how to sensibly combine translucent LSR3DP façade panels in a coherent façade assembly is, therefore, still unsolved. The present work aims to find an answer to this particular question.

1.4 OVERARCHING APPROACH

Connections play a crucial role in a building façade, as they must fulfil a wide array of delicate functions, such as ensuring waterproofing and air tightness, preventing condensation, avoiding thermal bridges, accommodating thermal dilatation and movements of the base structure. To meet high-quality standards, the building industry has progressively developed highly engineered solutions based on dry-mounted components (Knaack et al., 2007). The hypothesis presented in this article is that some of these solutions can be used to assemble translucent LSR3DP façade panels. This pragmatic approach "liberates" the 3D-printed component from the burdensome task of integrating performative connections and delegates the functionality to a highly tested and specifically designed solution. The present work focuses on one particular solution, namely a standard post and beam curtain wall system. The post and beam curtain wall system is traditionally used in combination with infill panels (either IGUs or opaque panels). It usually includes (i) a structure consisting of mullions and transoms, (ii) a clamping mechanism made of two aluminium profiles screwed to one another, (iii) a set of EPDM gaskets, which interpose between the aluminium profiles and the infill panels (FIG. 1A). In the present framework, the infill panels are substituted by bespoke LSR3DP panels (FIG. 1B). The result is a hybrid façade, which combines the customisation possibilities of 3DP with the performance reliability of standard curtain wall systems. For simplicity, from now on, this concept will be addressed as "3D printed Curtain Wall System" (3DPCWS).

FIG. 1 A) Standard post and beam curtain wall system B) Initial prototype constructed to assess the idea of combining standard curtain wall connections and LSR3DP façade panels.

This concept has been assessed by performing two different and complementary experiments.

(i) The first experiment aimed to evaluate the 3DPCWS from a functional standpoint. In particular, it aims to understand whether the standard curtain wall connection system still upholds its performance when the traditional infill panel is replaced with a bespoke 3D-printed component. Standard systems are meant to be combined with panels whose surfaces are flat. The gasket is designed to compress evenly against the flat panel under the force of the pressure plate, reducing air infiltration and preventing water penetration. A 3D-printed surface, however, features a certain rugosity derived from the deposition of the material, one layer on top of the other. As a consequence, if the flexibility of the gasket is unable to fill the groves of the layered surface, air and water can penetrate, compromising the performance of the façade itself. This possibility has been verified through an experiment consisting of constructing and testing a 1 m^2 façade mock-up. The mock-up has been tested for air permeability (SN EN 12153:2000 (*EN 12153*, 2000)) and water tightness (SN EN 12155:2000 (*EN 12155*, 2000)) in the facilities of Lucerne University of Applied Science and Arts (HSLU). Other technical requirements, such as wind and fire resistance, are not addressed in this study, as they fall within the capabilities of 3D printing technology. Wind resistance can be managed through an infill panel design with sufficient structural strength, while fire resistance is primarily determined by the properties of the materials selected. The Testing Laboratory Building Envelope and Civil Engineering of Lucerne University of Applied Sciences and Arts is authorised by the Swiss accreditation body (STS 0209) for air permeability and water tightness tests according to SN EN 13830:2003 (*EN 13830*, 2003). The experiment aims for a quantitative result.

(ii) The second experiment aimed to evaluate the 3DPCWS from an architectural perspective. It consists of developing a design case study that is able to express the system design potential. The case study corresponds to a single-storey building façade. It materialises in a large-scale demonstrator that integrates a façade mock-up and an enclosed space that offers the visitor an architectural experience. The development of the case study involved (i) the design of a timber substructure, (ii) the design of two LSR3DP façade panels, (iii) the façade connection detailing using different standard curtain wall solutions, (iv) the fabrication of the different components, (v) the demonstrator assembly. The process of developing a design case study aims to produce a qualitative rather than quantitative result.

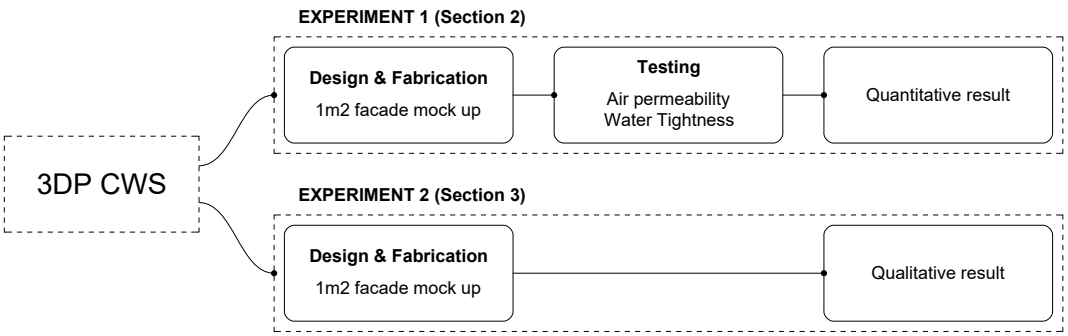

FIG. 2 Diagram summarising the process designed to validate the overarching approach.

2 EXPERIMENT 1 – AIR PERMEABILITY AND WATER TIGHTNESS TEST

2.1 METHOD

The following section describes the experiment that has been designed to assess the 3DPCWS from a functional perspective. The experiment tests the connections of a façade assembly for air permeability and air tightness. The aim of the test is not to give a resolutive answer but rather a preliminary indication of whether this approach can be used for industrial applications. Based on this study, further tests will need to be conducted to validate solutions developed for specific architectural projects. The following chapters include a description of the test specimen (2.1.1), a description of the testing facility (2.1.2), and information about the testing procedure (2.1.3 - 2.1.4).

2.1.1 LSR3D printed specimen and façade assembly

Air permeability and water tightness tests are generally performed on non-standard façade solutions to allow their use in specific architectural projects. The testing procedure – defined by SN EN 12153:2000 (*EN 12153*, 2000) and SN EN 12155:2000 (*EN 12155*, 2000) – requires testing the solution in the same configuration that will be used in the building assembly. In the present case, however, the test is not framed in the contingency of a specific architectural project but rather in a preliminary research scheme aimed at defining whether the approach has potential for architectural applications. This consideration has driven the design of the LSR3DP testing façade panel, conceived as a unitary 1 m x 1 m flat component (FIG.3A, 3B). The panel is characterised by a thickness of 50 mm, which is close to the maximum limit allowed by the selected standard curtain wall connection system (RAICO THERM+ H-I (*RAICO*, 2024)). The panel has an inside and an outside surface, separated by a folded zigzag infill, which provides structural rigidity. In the 3D printing process, the three elements that constitute the geometry emerge from one continuous toolpath. All design operations were executed using the software Rhinoceros 3D (*Rhinoceros 3D*, 2024).

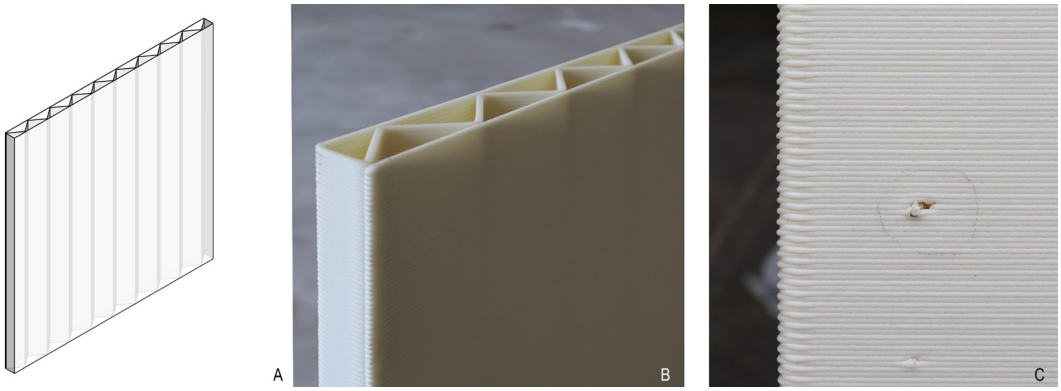

FIG. 3 A) Panel 3D model; B) 3D printed panel; C) Detail showing both the imperfection on the panel surface, corrected with silicon, and the increased rugosity on the panel's left and right edges due to material over-extrusion.

The façade panel was produced by SAEKI (*SAEKI Robotics*, 2024). The company received the panel 3D model from the author and created the robotic toolpath necessary for 3D printing. Production has been carried out using a custom-made LSR3DP set-up. The material chosen was ABS with 20% glass fibre. The choice of a non-transparent polymer was driven by wanting to 3D scan the panel after production to assess the precision of the 3D printing; an operation that would be more challenging in the case of transparent objects. The material extruder features three customisable heating zones for temperature control, which were set to 175, 190, and 225°C. The 3D printing toolpath featured a layer height of 2 mm, and the extruder material flow was tuned to achieve a 5 mm layer width. The superposition of the 3D model used for 3D printing and the one obtained through 3D scanning revealed no major deviation in the panel's global geometry. The panel surface presented minor (mm scale) imperfections due to fabrication errors (FIG. 3C). As the experiment focuses on the panel's edges interface, those imperfections were filled with a small amount of silicon to guarantee a perfectly tight panel surface. The left and right edges of the panel presented irregularities due to material over-extrusion. Although possibly harmful to the system performance, in this case, the irregularities were accepted as relatively common to the manufacturing technique and representative of LSR3DP elements (FIG. 3C).

The standard connection system selected for the experiment is RAICO THERM+ H-I (*RAICO*, 2024) (FIG. 1, FIG. 4). The system is an approved curtain wall solution specifically designed to interface the glazing with an internal load-bearing structure (steel, aluminium, timber...). Considering that the material has no influence on the experiment result, the timber option was selected for simplicity. The system features two drainage levels and pressure equalisation between the façade's interior and exterior space. It can adapt to different timber profile sizes, can be combined with panels up to 64 mm thick, and can hold panels up to 600 kg in weight. Performance-wise, combined with normal glazing, it guarantees a U value down to 0.76 W/(m^{2}K), air permeability classification AE (>600) according to SN EN 12152:2002 (*EN 12152:2002*, 2002), and water tightness classification RE 2100 according to SN EN 12154:1999 (*EN 12154:1999*, 1999).

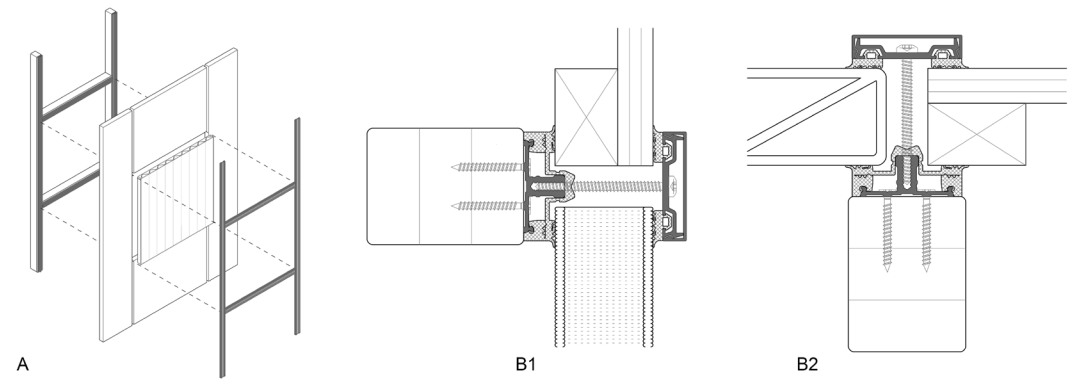

FIG. 4 A) Diagram of the façade assembly to be tested; B1) RAICO THERM+ H-I horizontal connection (transom); B2) RAICO THERM+ H-I vertical connection (mullion).

2.1.2 Description of the testing set-up

The main element of the set-up consists of a full-scale experimental rig from HSLU, which allows the testing of a façade assembly for air permeability and water tightness according to SN EN 12153:2000 (*EN 12153*, 2000) and SN EN 12155:2000 (*EN 12155*, 2000). The rig consists of a 1.5 m deep, 2 m wide

and 2.5 m high chamber. On one of the walls, the chamber has a door that allows access to the interior space for inspection. The opposite wall features a 2000 x 2500 mm opening, on which façade prototypes can be mounted and tested (FIG. 5). A system consisting of centrifugal fans, piping, and valves allows for air pressure control inside the chamber. Changeover flaps can switch the direction of the volume flow to create positive and negative test pressures. A negative test pressure in the chamber simulates the wind pressure on the outer side of the façade. In contrast, a positive test pressure in the chamber simulates wind suction on the outer side of the façade.

Outside the chamber, a water spray system is mounted, pointing at the position where the testing specimen gets installed. The system consists of spray nozzles arranged in a bar with a spacing of 400 mm. The nozzles are mounted 250 mm away from the façade and provide 120° cone-shaped water distribution. When active, the water spray system creates a constant water film on the surface of the specimen.

A set of measuring devices completes the set-up. In particular, (i) the differential pressure inside the chamber is assessed by three sensors (IDP 100, ICS Schneider Messtechnik, with measuring ranges respectively of ± 1000, ± 5000, and ± 10000 Pascal, max. deviation limit of 5% from the measured value). The sensors are located in the test chamber and are connected to the test chamber via pressure hoses so that the static pressure is determined independently of the air supply. (ii) The volume flow rate is measured by one transducer (TA 10 165 GE, measuring range 20 – 600 m^3/h, max. deviation limit of 5% from the measured value). (iii) The water flow is measured and adjusted by control valves (EP020R+MP, Belimo, measuring range 6-40 l/min, max. deviation limit of 10% from the measured value.) The measuring equipment is calibrated every two years according to the specifications of ISO 17025:2018 "General requirements for the competence of testing and calibration laboratories". The test facility is approved for accredited testing according to SN EN 13830:2003 (*EN 13830*, 2003).

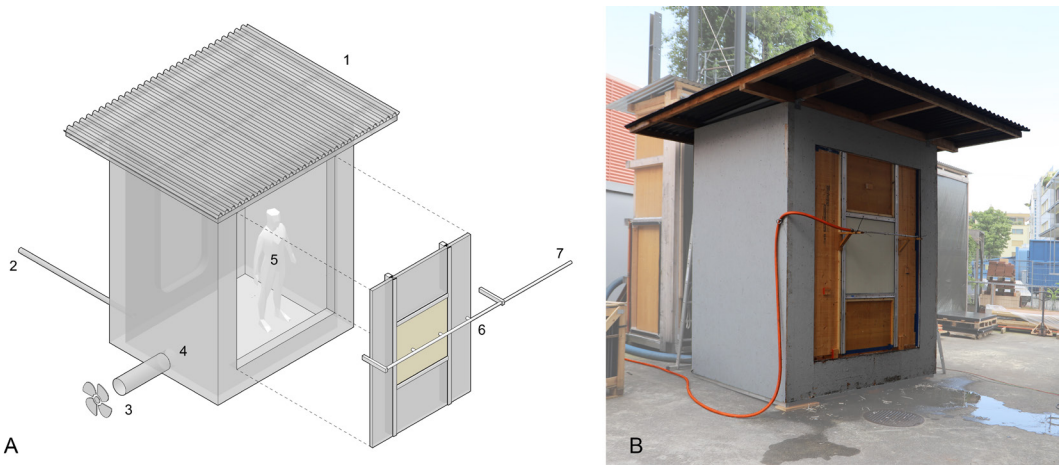

FIG. 5 A) Parts which compose the testing set-up. 1: Pressure cabine; 2: Pressure sensor; 3: Centrifugal fan; 4: Flow rate sensor; 5: Inspector; 6: Spray system; 7: Contro valve; B) Picture of the HSLU Testing Set-up in use.

The 3DP façade panel was installed in the centre of the HSLU experimental rig's opening (FIG. 5, FIG. 9A, FIG. 9B). The initial opening dimensions were adapted to the size of the panel by placing two timber mullions (GL24h, size: 60 x 100 x 2500 mm) spanning the whole aperture height, spaced centrally one meter away from one another. Among the mullions, two transoms were interposed,

also with a spacing of 1 m (GL24h, size: 60 x 100 x 945 mm). Around the panel, the aperture was closed using plywood sheets cut to size (FIG. 4). In the present configuration, consisting of continuous mullions interposed by transoms, the system is meant to channel any water seeping through the façade inside the mullions gasket and drain it through the lower aperture.

2.1.3 Air permeability test

The test was performed according to SN EN 12153:2000 (*EN 12153*, 2000). It consists of determining the airflow Q (mm^3/h), which passes through the façade assembly at specific pressure levels, and comparing it with the benchmark values defined by the standard. Before the test, three positive pressure pulses of 660 Pa are applied to stabilise the chamber; each pulse is held for a minimum of 3 seconds. The test itself consists of applying pressure inside the chamber, with sequentially increasing values corresponding to 50, 100, 150, 200, 300, 450, and 600 Pa. Each pressure level is held for a minimum time of 10 seconds. At each pressure level, the set-up allowed measuring Q_1 (m^3/h), meaning the global airflow passing through the testing chamber. This value is averaged over the measurement time and includes the airflow through façade assembly Q plus the chamber leakage Q_0. The chamber leakage was measured before starting, following the guidelines of EN 12153:2000 (*EN 12153*, 2000), which consists of performing an initial measurement after airtight-sealing the specimen. This procedure ensures that no air leakage is encountered at the junction between the plywood perimeter panels and the curtain wall system. Q is determined as Q_1-Q_0. The procedure is repeated two times, the first one with a positive pressure inside the chamber and the second one with a negative pressure (FIG. 6A). The air permeability of the façade can be assessed both in relation to the surface area of the façade fixed element (q_A) and in relation to the linear meter of closed joints (q_L). The first is calculated as:

$$q_A = Q/A = (Q_1\text{-}Q_0)/A(m^3/hm^2)$$

while the second is calculated as:

$$q_L = Q/L = (Q_1\text{-}Q_0)/L\ (m^3/hm^2)$$

A is the total specimen area, corresponding to 1 m^2, and L is the connection length, corresponding to 4 m.

The air permeability performance requirements and classifications for curtain walls are defined in the SN EN 12152:2002 (*EN 12152:2002*, 2002).

During the test, any airflow infiltration through the connections could be visualised by producing smoke at the interface between the panel and the gasket. This test was performed by a person standing inside the chamber while the pressure was applied, allowing the inspector to understand whether the filtration is uniform (i.e. structural to the system) or concentrates at specific points (i.e. due to errors during the façade assembly).

2.1.4 Water tightness test

The test was performed according to SN EN 12155:2000 (*EN 12155*, 2000). It consists of verifying that the façade is impermeable to water at specific negative pressure levels. In this case, positive pressure is not relevant, as wind suction on the façade doesn't increase the risk of water penetration (FIG. 6B). Before the test, three negative pressure pulses of 660 Pa are applied; each pulse is held for a minimum of 3 seconds. The test itself consists of two phases. First, the spraying system is activated, and the façade is completely sprayed with water for 15 min without any pressure inside the testing chamber. Second, pressure is applied inside the chamber, with sequentially increasing values corresponding to 50, 100, 150, 200, 300, 450, and 600 Pa. Each pressure level is held for a minimum time of 10 seconds. For each pressure level, an inspector inside the chamber checks whether water penetrates the assembly.

The amount of water to be sprayed is calculated as the façade element area multiplied by 2 l/(min·m^2). Therefore, the amount of water required for testing the façade assembly described above was:

$$T_{water} = 1m^2 * 2l/(min*m^2) = 2l/min$$

The water tightness performance requirements and classifications for curtain walls are defined in the SN EN 12154:1999 (*EN 12154:1999*, 1999).

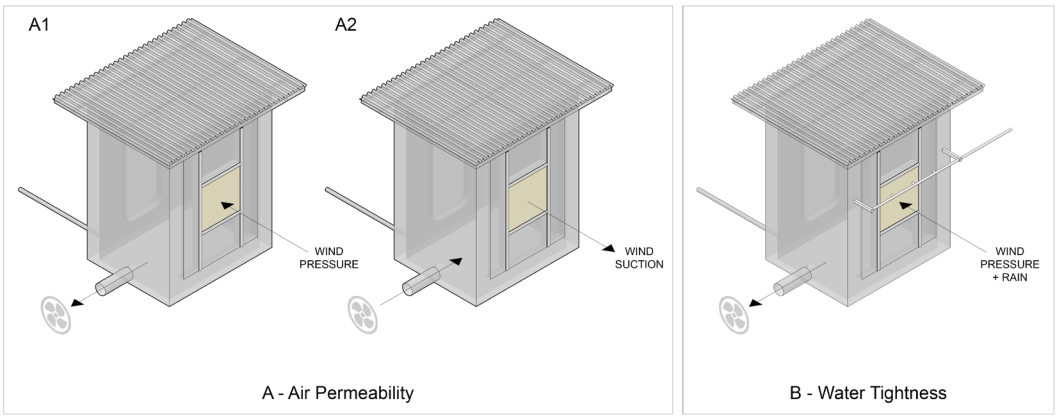

FIG. 6 Tests performed in the HSLU testing rig. A1) Air permeability with positive pressure, simulating air suction on the façade assembly; A2) Air permeability test with negative pressure, simulating wind pressure on the façade assembly; B) water tightness test with negative pressure, simulating wind pressure on the façade assembly.

2.2 RESULTS

2.2.1 Air permeability test

This chapter summarises the result of the air permeability test described in Chapter 2.1.3. The test lasted for about 24 minutes. FIG. 7 shows the progressively increasing pressure applied in the testing chamber, both in the positive and negative directions.

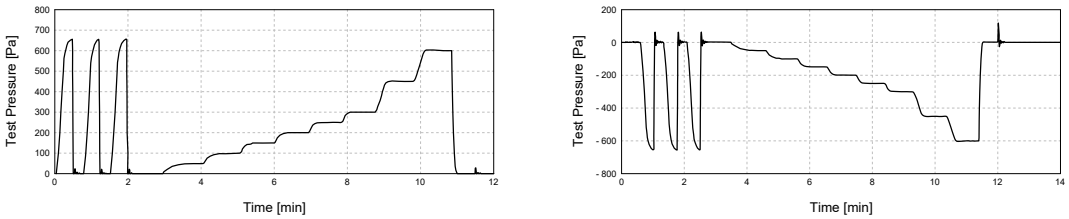

FIG. 7 A) Diagrams showing the positive pressure applied in the testing chamber progressively increasing over time. B) Diagrams showing the negative pressure applied in the testing chamber progressively increasing over time.

At specific pressure values (± 50, 100, 150, 200, 250, 300, 450, 600 Pa), the average airflow through the façade assembly Q (m^3/h) was measured. From those values, the façade permeability is derived, both in relation to the area of fixed element (q_A) and in relation to the linear meter of closed joints (q_L). Q and q_A have equal values because the specimen surface area corresponds to 1 m^2. Table 1 shows the values of Q, q_A, and q_L measured at each pressure level for both positive and negative pressure.

	Negative pressure								Positive pressure							
Test pressure [Pa]	**-600**	**-450**	**-300**	**-250**	**-200**	**-150**	**-100**	**-50**	**50**	**100**	**150**	**200**	**250**	**300**	**450**	**600**
Q (m3/h)	1.683	2.191	1.537	0.919	0.903	0.444	0.52	0	0.269	0.41	0.343	0.808	0.901	1.211	1.605	1.817
qA (m3/hm2)	1.683	2.191	1.537	0.919	0.903	0.444	0.52	0	0.269	0.41	0.343	0.808	0.901	1.211	1.605	1.817
qL (m3/hm)	0.421	0.548	0.384	0.23	0.226	0.111	0.13	0	0.067	0.103	0.086	0.202	0.225	0.303	0.401	0.454

TABLE 1 Table showing, for each positive and negative pressure level: 1) The m^3 of air flowing through the façade assembly per hour (Q). 2) The m^3 of air flowing through the façade assembly per hour relative to the façade surface area (qA). 3) The m^3 of air flowing through the façade assembly per hour reactive to the façade linear meter of closed joints (qL).

The results were assessed according to the SN EN 12152:2002 (*EN 12152:2002*, 2002), which classifies façade air permeability within four categories of increasing efficiency level (A1, A2, A3, A4). For each category, the standard defines the maximum air permeability value allowed at each pressure level. FIG. 8A, 8B, 8C, and 8D show the results in relation to the categories thresholds. To achieve a certain category classification, the value points corresponding to all pressure levels (positive and negative) have to be below the corresponding category line in the diagram. For categories A1, A2, and A3, only pressure values up to ± 150, ± 300 and ± 450, respectively, are relevant.

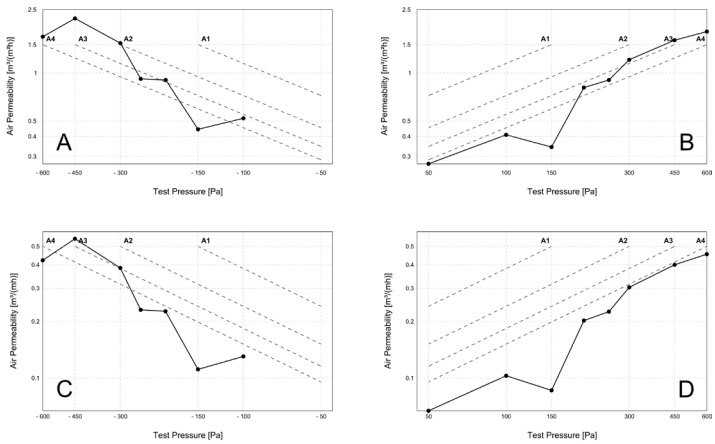

FIG. 8 Diagrams showing the results of the air permeability test in relation to the benchmark values defined by SN EN 12152:2002. A and B show qA values for negative and positive pressure, respectively. C and D show qL values for negative and positive pressure, respectively.

When evaluated with the "air flow through the area of fixed element" criteria (q_A), the façade specimen classifies as A1, as the value of 1.537 m^3/m^2h corresponding to the pressure level -300 Pa is just above the threshold for category A2, which is 1.5 m^3/m^2h. When evaluated with the "air flow through closed joints" criteria (q_L) however, the façade classifies in category A2, as all the values are below the threshold for category A2. The façade does not classify as A3, as the values corresponding to the pressure levels -300 and -450 Pa are above the A3 threshold. For q_A and q_L, the evaluation criteria resulting in the better category can be selected. Therefore, the façade specimen classifies as A2.

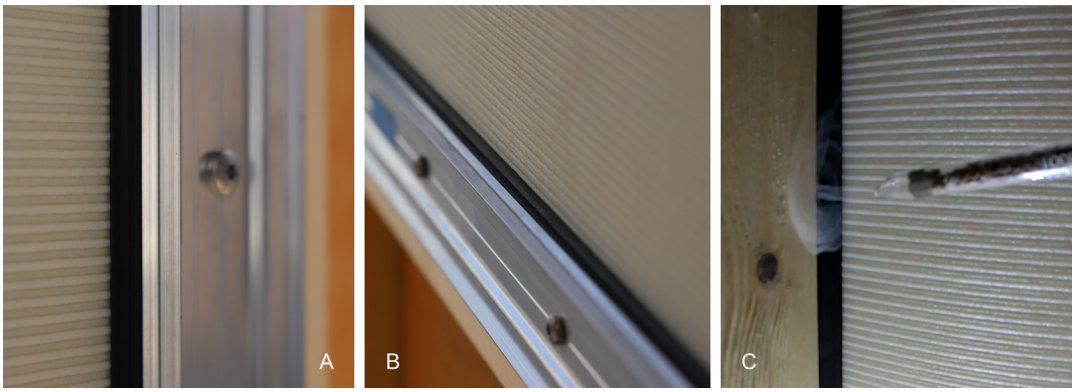

FIG. 9 A) Test vertical connection (mullion); B) A) Test horizontal connection (transom); C) Visualization of the airflow. With positive pressure, the smoke gets "sucked" through the vertical connection. This phenomenon does not occur at the horizontal connection.

During the test, the airflow through the connections was visualised by producing smoke at the interface between the 3DP panel and the gasket. At the top and bottom sides, no air movement could be observed. On the left and right edges, however, a flow in the horizontal direction was clearly visible (FIG. 9C), suggesting that the layered texture of the 3DP panel, to some extent, affects the functionality of the vertical gaskets. The air movement was uneven through the edge, suggesting that some imperfection in the façade assembly might have also come into play.

2.2.2 Water tightness test

This chapter summarises the result of the air permeability test described in chapter 3.1.4. The test had a total duration of 55 minutes. FIG. 10 shows the negative pressure in the testing chamber, progressively increasing during the test, and the constant water flow sprayed on the outside of the specimen.

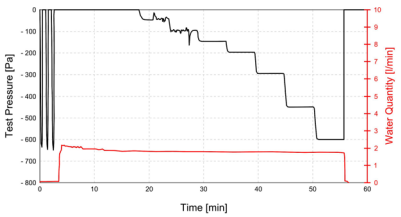

FIG. 10 Diagrams showing the negative pressure applied in the testing chamber progressively increasing over time and the constant water flow sprayed on the outside of the façade.

For the whole test duration, three people stood inside the testing chamber, inspecting the façade assembly. No water penetration was observed throughout the duration of the test. The results were assessed according to the SN EN 12154:1999, which classifies façades' water tightness within four categories of increasing efficiency level (R4, R5, R6, R7). The façade specimen is classified in category R7.

3 EXPERIMENT 2 – EXPLORING THE SYSTEM'S ARCHITECTURAL POTENTIAL

The previous chapter describes the experiment designed to validate the concept of a 3DPCW from a functional standpoint. The experiment aimed for a quantitative result, namely, the system classification of air permeability and water tightness. This analysis is not without limitations. On the one hand, being a preliminary study, it produces numerical information on one single CW system (RAICO THERM+ H-I), even though countless standard CW systems exist on the market and could be used with the same approach. On the other hand, focusing on functionality, the study leaves behind the possibility of exploring the architectural and tectonic potential of this novel approach. The process described in the following chapter has been specifically designed to fill this gap and should be considered as a complementary study. The approach is rather oriented to a qualitative result. In this case, the vocabulary of standard CW solutions has been expanded, considering that all solutions adapted to LSR3DP façade panels would function similarly. Also, the focus has been shifted to demonstrating the design possibilities offered by the novel façade system.

3.1 METHOD

The experiment presented in this section consists of the design and fabrication of a large-scale demonstrator. The large-scale demonstrator corresponds to a single-storey building façade mock-up, including two organically shaped LSR3DP panels. The panels have a rectangular outline, each measuring 2 m in height, 1 m in width, and having a variable thickness from 10 mm to

35 mm. Within the mock-up, the panels span from floor to ceiling and are reciprocally connected by a central mullion. Behind the façade, the roof and the floor extend for 1 m, creating a 2 m^2 accessible space. The total height of the mock-up was set at 2 m rather than a regular floor height (2.4 m to 2.7 m) to limit the panel's 3D printing time. All the components composing the façade's structure (floor, roof, mullion, upper and lower façade horizontal edges) are made of timber. The detailing of the interface between the panels and the timber substructure was carried out using the solution set offered by the company RAICO®. Three different details were developed: the connection between the panels and the roof (FIG. 11B1), the connection between the panels and the floor (FIG. 11B3), and the reciprocal connection between the panels (FIG. 11B2).

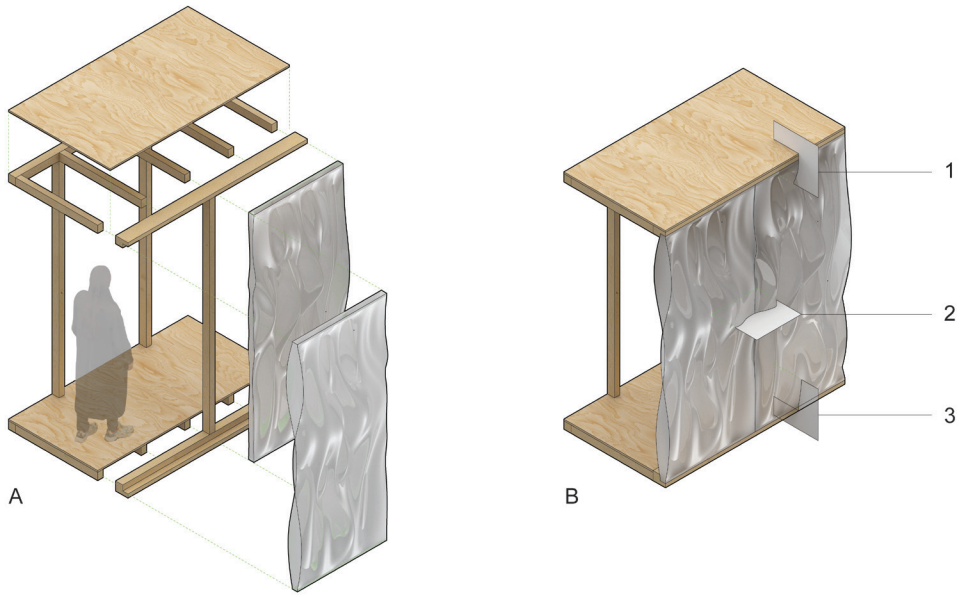

FIG. 11 A) demonstrator constructive logic; B) types of connections studied: 1: façade - roof connection; 2: panel to panel connection; 3: façade to floor connection.

3.2 RESULTS

3.2.1 Design of the LSR3DP panels

One of the advantages of 3D printing is the possibility of tailoring the geometry and targeting specific material performances. It has been shown, e.g., that different panel infills lead to different thermal performances (Piccioni, Leschok, Lydon, et al., 2023) as different degrees of light transmission and solar gain can be achieved through different printing patterns on the outside surface (Piccioni, Leschok, Grobe, et al., 2023) (Cheibas, Piccioni, et al., 2023). The present study, however, does not focus on building physics but rather on the panel's connections and the system tectonic. Therefore, in the design of the two mock-up panels, both infill and surface patterns have been simplified to reduce material use and printing time. Besides this fact, the connection strategy outlined here is

compatible with the guidelines offered in the aforementioned studies, focusing on producing high-performance LSR3DP façade panels (e.g. maximizing the number of air cavities within the infill to improve the panel U value).

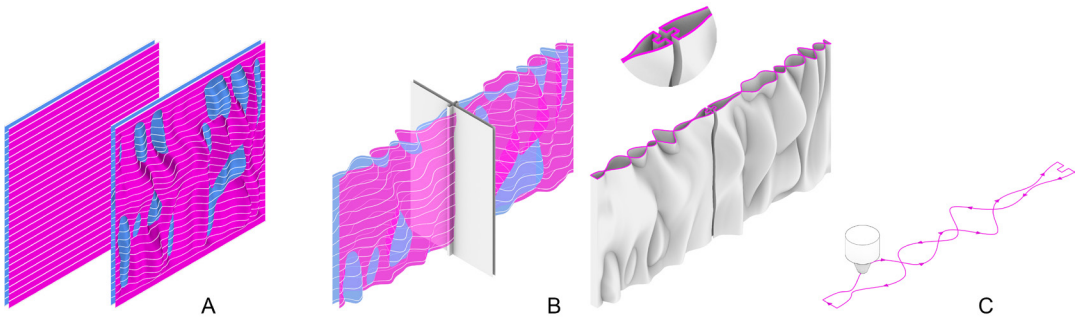

FIG. 12 3DP panels design logic. A) Perlin noise applied to two parallel surfaces; B) Production of the connection detail; C)Toolpath consisting of one continuous smooth curve.

A first guideline for the current design process was based on exploring new aesthetics allowed by 3DP, creating a geometry that could not be made by any other means. Given those prerequisites, the concept for the façade global geometry resulted in a volume defined by two intersecting free-form surfaces (FIG.12A). The design process was held within Rhinoceros 3D and Grasshopper, a 3D modelling environment that allows parametric operations. The global façade geometry is created by applying a Perlin noise (Perlin, 1985) distortion to a couple of rectangular, flat, parallel B-rep surfaces. The multiple intersections between the two surfaces are meant to provide rigidity to the panel. A second design criterion for the current demonstrator has been production speed optimisation. To allow higher velocity during printing, avoiding vibration and consequential quality loss, the 3D printing toolpath needs to avoid kinks and sharp edges. When sliced horizontally, the chosen geometry results in a series of smooth cross-sections (FIG.12C).

3.2.2 Connection detailing

In the previous experiment, the façade concept consisted of continuous mullions separated by transoms. In the present case, a different configuration was explored. The façade scheme consists of two continuous transoms on the upper and lower limits of the façade, between which the mullions are interposed. In the present configuration, the system is meant to channel any water seeping through the façade inside the lower transom gasket and drain it through specific apertures.

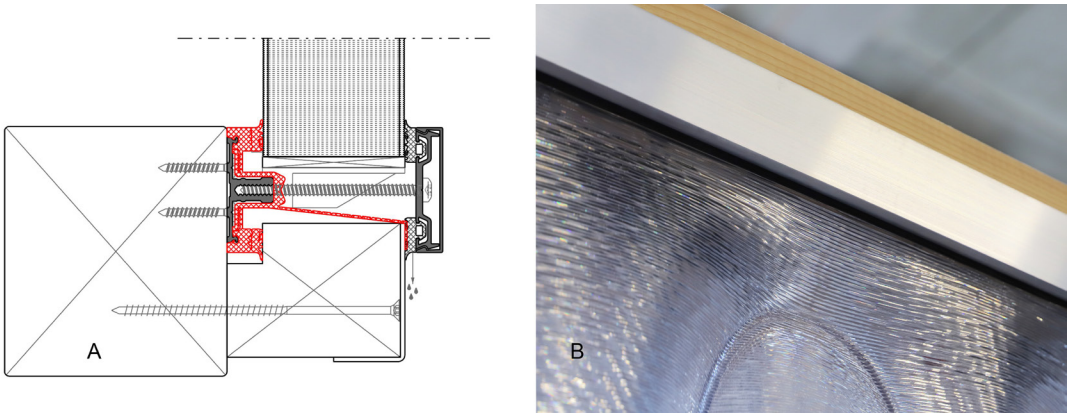

FIG. 13 A: façade-floor connection detail; B: Close-up of façade-roof connection in the final demonstrator.

For the panel's horizontal connections, corresponding to the façade's upper and lower edges, the same connection type was adopted as used in experiment 1 (RAICO THERM+ H-I). The pattern characterising the panels was designed to progressively fade towards the upper and lower edges, transitioning smoothly from an organic surface to a flat one. This way, the flat portion of the panel could be effectively clamped between the two aluminium profiles and EPDM gaskets of the standard CW system (FIG. 13). For the lower detail, a special gasket was chosen to create an internal gutter able to collect and evacuate any water seeping through the connections and draining through the mullions (FIG. 13A, element in red).

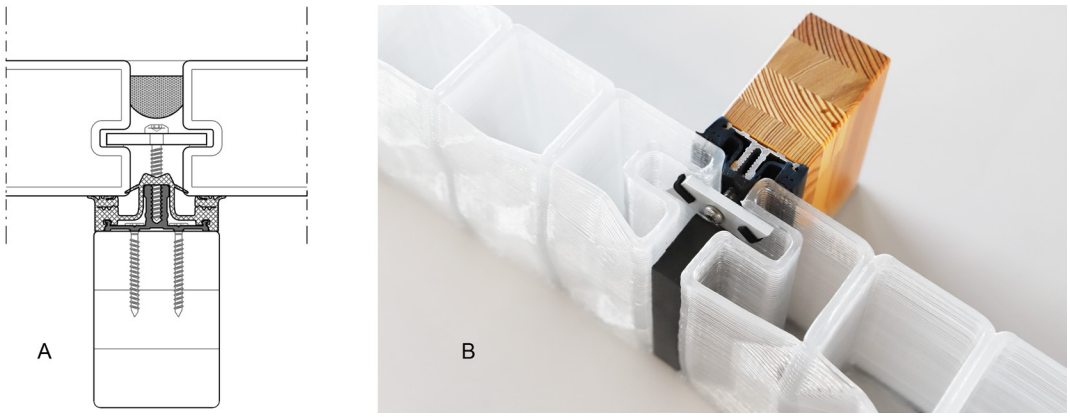

FIG. 14 A: Panel-to-panel vertical connection detail; B: Panel-to-panel vertical connection, prototype (wet or dry sealant missing).

A different solution was adopted for the vertical connection. The curvy pattern characterising the façade design is continuous throughout the two panels. Respecting the pattern continuity required a strategy to limit the visual impact of the vertical connection. This goal was achieved by hiding the fixation to the timber mullion within the thickness of the panel. This involved adopting a different solution compared to the one used in experiment 1. The solution consists of a special curtain wall detail based on an aluminium profile, EPDM gasket, punctual fasteners (toggles), and wet or dry sealant (RAICO THERM+ H-I Structural glazing SG2). This detail is commonly used to avoid additional frames on the outside of the façade and to achieve a flush glass surface. The toggles are generally inserted in a groove specifically manufactured in the IGU or panel edge. A similar groove was designed and produced on the left and right edge of the 3D-printed panel (FIG. 14). The 3D-printed infill panel does not require structural silicone bonding for its functionality. This presents a clear advantage over traditional SG glass systems, which rely on bonding performance control, testing, and other stringent requirements.

3.2.3 Fabrication of the LSR3DP panels

For the 3D printing to be executed, the geometrical information of the 3D model needed to be translated into a toolpath, meaning a series of positions the robot has to reach progressively during fabrication. This operation was performed within Rhinoceros and Grasshopper, the same parametric environment used for all design operations. The workflow consisted of (i) slicing the 3D model vertically to obtain parallel polylines (the 3D printing layers) spaced 2 mm apart; (ii) dividing the polylines into points, spaced approximately 5 mm apart; (iii) assigning to each point an XY plane, which the robot could interpret as a position instruction. The communication between the 3D modelling environment and the machine was established through COMPAS_RRC (*COMPAS RRC*, 2024) using a JavaScript Object Notation (JSON) as an intermediary file format.

The two LSR3DP panels were produced in the Robotic Fabrication Lab of ETH Zurich. The 3DP set-up consisted of a CEAD thermoplastic extruder (CEAD, 2024) attached to an ABB 4600 robotic arm, which, in turn, was attached to a gantry system. This particular configuration allowed for the great cinematic possibilities required to 3D print large-scale components. The CEAD extruder works with different types of thermoplastics and must be fed with material in the form of pellets. For the present case, transparent Polyethylene Terephthalate Glycol (PETG) was employed. The material has a low warping tendency and is, therefore, widely used in LSR3DP applications. Before fabrication, the material was dried for 4 h at 60°C in a VisMec Dryplus 50 dryer to remove moisture. The extruder features four customisable heating zones for temperature control and a custom-made cooling device that releases compressed air of 0.6 bar pressure. The heating zones were set respectively to 215, 225, 235, and 245°C, and the cooling device was turned on during printing. A 3 mm nozzle was used for extrusion, and the material flow was regulated to achieve a wall thickness of 5 mm.To reduce the risk of warping and improve the adhesion between the panels and the 3D printing groundwork during fabrication, a 50 mm brim layer was added at the base of the panels. The toolpath length of the two panels corresponded to 2556 m and 2831 m. Since the robot velocity was set to 70 mm/s, printing time resulted in 10 hours and 8 minutes for the first panel and 11 hours and 14 minutes for the second panel. For safety reasons, the set-up was run in manual mode, meaning, an operator had to hold the safety button on the ABB flex pendant during the whole fabrication process. For this reason, the printing sessions were interrupted multiple times, leading to imperfections in the panel's 3D-printed surface. The weight of the 3DP panels resulted in 31.4 kg for the first and 34.8 kg for the second panel, meaning an average of 16.5 kg/m^2. Each panel could easily be handled by two people during the assembly operations.

3.2.4 Fabrication of the timber substructure and assembly

The timber substructure was produced using conventional carpentry techniques. The roof and the floor were produced using two sheets of plywood 18 mm thick, stiffened by a timber frame made of 80x60 mm planks. The mullion and the two columns supporting the roof were produced using 80x60 mm timber planks. In contrast, the upper and lower façade limits, which are characterised by a more complex cross-section, were produced by glueing multiple planks of different cross-sections. The different timber components were assembled using a nailer powered by a compressor. After the construction of the timber substructure, the façade system (aluminium profiles, EPDM gaskets, pressure plates, 3DP panels...) was assembled in a timeframe of two hours (FIG. 15).

FIG. 15 2 m x 2 m x 1 m single-storey building façade mock-up consisting of two 3DP façade panels integrated into a timber substructure with off-the-shelf curtain wall connections

4 CONCLUSION

The present study focuses on the problem of connections in LSR3DP façades. It builds upon the general hypothesis that experimental solutions can benefit from hybridisation with standard, highly tested products to find an easier way into real-world architecture. In this framework, the study introduces the idea of using conventional curtain wall connections to join highly customised 3DP façade panels. The concept was evaluated both from a functionality and from a design standpoint.

In the first instance, an experiment was performed to classify the system for air permeability and water tightness.

Regarding air permeability, the system was classified in category A2 according to SN EN 12152:2002. The standard CW system used in the experiment (RAICO THERM+ H-I), when combined with IGUs or opaque panels, is classified in a higher category (AE (>600)). This means that the substitution of IGUs with LSR3DP does indeed have a slightly negative impact on the connection's performance, presumably due to the horizontal grooves in the 3DP surface derived from the layered deposition of the material. Besides the performance loss, A2 classification should be considered a positive result, acknowledging that this is a preliminary study aimed to define whether this approach can be used in architectural projects. Façades classified as A2 can, in fact, be used in architecture where the expected wind dynamic pressure is moderate. The use of SN EN 12152:2002 classified system in relation to wind dynamic pressure is regulated by the SIA 329 (*SIA 329*, 2018) (*SN 520329*, 2018). In case a project requires it, further studies will need to address the improvement of the system's air permeability performance. In this regard, three alternative approaches are suggested. First, the test could be repeated, increasing the pressure on the clamping mechanism. This could be achieved by,

e.g. increasing the number of screws that connect the pressure plate to the mullions and transoms. Second, a custom gasket could be developed, characterised by greater thickness and higher flexibility. Third, special attention could be paid to the fabrication of the panel's edges, adjusting parameters dynamically (e.g. velocity) to achieve a smoother interface with the gasket. As stated in section 2.2.1, the performance loss concerns only the connections that meet the 3D-printing layers perpendicularly; therefore, those measures could be limited to those particular points.

Regarding water tightness, the system was classified in category R7 according to SN EN 12154:1999. R7 is a highly performative category, and it is suitable for the majority of architectural projects. The standard CW system used in the experiment (THERM+ H-I), in combination with IGUs, is certified by RAICO as RE 2.100, meaning it can withstand water penetration with a pressure up to 2100 Pa. Verifying whether the system performs equally to the same pressure level in combination with LSR3DP façade panels is outside the scope of this study. In terms of water tightness, the system does not require any improvement or further testing.

In the second instance, an experiment consisting of a design case study was developed to assess the system from a broader perspective. From an aesthetical standpoint, the hybrid tectonic, which arises from the combination of conventional façade construction on the one hand and digitally designed and fabricated custom elements on the other, offers an exciting territory for designers to explore. In this regard, the present work aims to present a general methodology and inspire further research. Future works on this line could either use the façade solutions detailed in this paper, exploring new designs and functionalities for the 3D-printed panels or abstract the overarching logic and adapt it to other solutions provided by the façade construction industry (e.g. unitised façade system). Moreover, future research should tackle how this approach could be adapted to the different situations of increased complexity which commonly arise in building façade design (corner detail, presence of apertures like doors and windows).

Another consideration concerns the interdependence – implicitly entailed in this approach – between the geometrical freedom provided by LSR3DP and the limits imposed by the underlying substructure. With 3D printing, one can easily produce façade panels characterised by a curved boundary. However, increasing the complexity of the panel boundary naturally means producing the same effect on the underlying substructure, a condition which might not always be desirable due to fabrication constraints. This fact needs to be carefully taken into account in the design phase. The demonstrator presented in this paper studied the case of a simple façade composed of straight mullions and transoms arranged in a planar configuration. The geometrical complexity allowed by 3D printing has been celebrated by producing a custom texture on the panel surface rather than creating a complex global geometry. Future studies should go beyond this condition and explore more complex configurations characterised by single or double curvature. A first option worth exploring in this framework is a façade whose global geometry is defined as a ruled surface. This condition could still be achieved using straight mullions and transoms. A further step in this direction would be introducing curved elements for the substructure. This might be possible with different state-of-the-art technologies depending on the materiality of the components. This option would allow taking full advantage of the geometrical complexity allowed by 3DP in creating complex shapes for the panels and consequentially expand the set of architectural typologies achievable by this means (e.g. domes, grid-shells).

Acknowledgements

ETH RFL: Michael Lyrenmann, Philppe Fleishmann, Luca Petrus. ETH MAS dFab: Aejmelaeus-Lindstrém Petrus. HSLU: Bruno Marty. Raico: Josef Erni, MArtin Eberhard. Saeki: Matthias Leshock

References

Al Jassmi, H., Al Najjar, F., & Mourad, A.-H. I. (2018). Large-Scale 3D Printing: The Way Forward. *IOP Conference Series: Materials Science and Engineering*, *324*. https://doi.org/10.1088/1757-899X/324/1/012088

CEAD. (2024). *CEAD Group*. CEAD | Large Scale Additive Manufacturing. https://ceadgroup.com/

Cheibas, I. (2023). *Additive Manufactured Facade*. https://doi.org/10.3929/ethz-b-000648606

Cheibas, I., Lloret-Fritschi, E., Piccioni, V., Leschok, M., Dillenburger, B., Schlüter, A., Gramazio, F., & Kohler, M. (2023). *Thermoplastic large-scale 3D printing of a light-distribution and fabrication-informed facade panel*. https://doi.org/10.3929/ETHZ-B-000639445

Cheibas, I., Perez Gamote, R., Önalan, B., Lloret-Fritschi, E., Gramazio, F., & Kohler, M. (2023). Additive Manufactured (3D-Printed) Connections for Thermoplastic Facades. In *Trends on Construction in the Digital Era* (Vol. 306, pp. 145–166). Springer International Publishing. https://doi.org/10.1007/978-3-031-20241-4_11

Cheibas, I., Piccioni, V., Lloret-Fritschi, E., Leschok, M., Schlüter, A., Dilllenburger, B., Gramazio, F., & Kohler, M. (2023). Light Distribution in 3D-Printed Thermoplastics. *3D Printing and Additive Manufacturing*. https://doi.org/10.1089/3dp.2023.0050

COMPAS RRC. (2024). https://compas-rrc.github.io/compas_rrc/latest/

EN 12152:2002—Curtain walling - Air permeability - Performance requirements and classification; German version. (2002).

EN 12153:2000—Curtain walling—Air permeability—Test methods; German version. (2000).

EN 12154:1999—Curtain walling - Watertightness - Performance requirements and classification; German version. (1999).

EN 12155:2000—Curtain walling—Watertightness—Laboratory test under static pressure; German version. (2000).

EN 13830:2003—Curtain walling—Product standard; German version. (2003).

Engelsmann, S., Spalding, V., & Peters, S. (2010). *Plastics in Architecture and Construction* (Birkhäuser).

Fleckenstein, J., Bertagna, F., Piccioni, V., Fechner, M., Düpree, M., DAcunto, P., & Dörfler, K. (2023). *Revisiting Breuer through Additive Manufacturing: Passive solar-control design strategies for bespoke concrete building envelope elements*. 527–538. https://doi.org/10.52842/conf.ecaade.2023.1.527

Herzog, T., Krippner, R., & Lang, W. (2004). *Facade construction manual* (1st ed). Birkhauser-Publishers for Architecture.

Knaack, U., Bilow, M., Klein, T., & Auer, T. (2007). *Fassaden: Prinzipien der Konstruktion*. Birkhäuser Verl.

Leschok, M., Cheibas, I., Piccioni, V., Seshadri, B., Schlüter, A., Gramazio, F., Kohler, M., & Dillenburger, B. (2023). 3D printing facades: Design, fabrication, and assessment methods. *Automation in Construction*, *152*, 104918. https://doi.org/10.1016/j.autcon.2023.104918

Mungenast, M. B. (2019). *3D Printed Future Facade*.

Naboni, R., & Jakica, N. (2022). Additive manufacturing in skin systems: Trends and future perspectives. In *Rethinking Building Skins* (pp. 425–451). Elsevier. https://doi.org/10.1016/B978-0-12-822477-9.00004-8

Perlin, K. (1985). *An image synthesizer*.

Piccioni, Leschok, M., Lydon, G., Cheibas, I., Hischier, I., Kohler, M., Gramazio, F., & Schluter, A. (2023). *Printing thermal performance: An experimental exploration of 3DP polymers for facade applications*. https://doi.org/DOI 10.1088/1755-1315/1196/1/012063

Piccioni, V., Leschok, M., Grobe, L. O., Wasilewski, S., Seshadri, B., Hischier, I., & Schlüter, A. (2023). Tuning the Solar Performance of Building Facades through Polymer 3D Printing: Toward Bespoke Thermo-Optical Properties. *Advanced Materials Technologies*. https://doi.org/10.1002/admt.202201200

RAICO. (2024). https://www.raico.de/

Rhinoceros 3D. (2024). https://www.rhino3d.com/

SAEKI Robotics. (2024). https://www.saeki.ch/

Seshadri, B., Cheibas, I., Leschok, M., Piccioni, V., Hischier, I., & Schlüter, A. (2021). Parametric design of an additively manufactured building facade for bespoke response to solar radiation. *Journal of Physics: Conference Series*. https://doi.org/10.3929/ethz-b-000521182

SIA 329. (2018).

SN 520329. (2018).

Strauß, H. (2013). *AM Envelope / The potential of Additive Manufacturing for façade construction*. https://doi.org/10.7480/abe.2013.1.386